Mercury-Ion Clock Based on a Linear Multi-Pole Ion Trap

J. D. Prestage,[1] R. L. Tjoelker,[1] and L. Maleki[1]

Buffer-gas-cooled clocks rely on large numbers of ions, typically $\sim 10^7$, optically pumped by a discharge lamp at scattering rates of a few photons per second per ion. To reduce the second Doppler shift from space-charge repulsion of ions from the trap node line, novel multi-pole ion traps are now being developed wherein ions are weakly bound with confining fields that are effectively zero through the trap interior and grow rapidly near the trap electrode "walls."

I. Multi-Pole Linear Ion Traps

Higher pole traps have been used as a tool in analytical chemistry to study ion-molecule low-energy collisions and reactions. Octopole rf electrodes act as guides to transport ions from one location to another in similar applications. These applications involve very low densities of ions where space-charge interactions within the ion cloud are inconsequential. Ions are detected directly with a channeltron electron multiplier. Because ions in a multi-pole rf trap spend relatively little time in the region of high rf electric fields, there is very little rf heating, and low-temperature collisions can be studied [1,2].

The pseudo-potentials for quadrupolar trapping fields are equivalent to a uniform background pseudo-charge with a consequence that (cold) ion clouds fill the trap with uniform density [3]. In lamp-based clock applications, most of the second-order Doppler shift for large ion clouds in a linear quadrupole trap is a consequence of the space-charge coulomb repulsion force that results from confining ions of like charge in a relatively small volume. These repulsive forces are balanced by the ponderomotive forces generated by ion motion in the rf electric field gradient. For large ion clouds, most of the motional energy is stored in the micro-motion necessary to generate the force to balance the space-charge repulsion. For a typical cloud, buffer gas cooled to 500 K, the second Doppler shift from rf micro-motion can be up to three times the secular motion contribution to the energy [4].

Since higher pole traps have not previously been used in clock applications, we shall review some properties of large ion clouds in multi-pole traps, where space-charge effects are non-negligible. The pseudo-potential, $V^*(r)$, for a particle of charge q and mass m inside the linear multi-pole trap with $2k$ electrodes is given by [1]

$$V^*(r) = \frac{k^2}{16} \frac{q^2 U_0^2}{m \, \Omega^2 \, r_0^2} \, \hat{r}^{2k-2} \equiv \frac{k^2}{8} \, m\omega^2 r_0^2 \hat{r}^{2k-2}$$

The operating rf frequency is Ω radians per second; the trap inner radius is r_0; and the amplitude of the rf voltage applied to each rod is $U_0/2$. (The peak voltage between neighboring trap electrodes is U_0.) The normalized distance $\hat{r} = r/r_0$. The equation of motion for an ion in the time-varying harmonic potential of a linear quadrupole is the Mathieu equation [3], and it forms the basis for mass selectivity in rf mass spectrometers, when combined with a static electric field. The electric field growth with radial distance from the centerline is assumed to be linear with a constant growth in strength out to the trap electrodes. The Mathieu equation and its solutions determine those charges-to-masses, q/m, whose trajectories are stable for the given trap dimensions, operating frequencies, applied voltages, etc. Unstable trajectories can result (in harmonic linear traps) when the extent of a particle's oscillatory micro-motion is comparable to its distance to the trap center. This can be formulated as an adiabaticity requirement. Accordingly, for stable trapping, the change in the electric field amplitude over the extent of the particle's oscillatory micro-motion must be less than the field amplitude [1,3].

In a higher pole trap, the rapid growth of the trapping fields near the electrodes can violate the adiabaticity requirement imposed on the motion of a charged particle to ensure stable trapping. By numerical computation of single particle trajectories [1], it is found that as long as the adiabaticity parameter

$$\eta = \frac{2q \, |\nabla E_0|}{m\Omega^2} = k(k-1)\frac{qU_0}{m\Omega^2 r_0^2}\hat{r}^{k-2} \leq 0.3 \equiv \eta_{\max}$$

then particles will be trapped in a stable orbit. In practice, this means that for a particle to remain bound during its trajectory it cannot travel outside the radius

$$R_{\max} = r_0 \left[\frac{0.3}{k(k-1)} \frac{m\Omega^2 r_0^2}{qU_0} \right]^{\frac{1}{k-2}}$$

where $k > 2$. The well depth in a multi-pole trap can be defined as the value of the pseudo-potential at $R_{\max}$,

$$V^*(R_{\max}) = \frac{m\Omega^2 r_0^2}{16} \left[\frac{\eta_{\max}}{k-1} \right]^{2\frac{k-1}{k-2}} \left[\frac{1}{k} \frac{m\Omega^2 r_0^2}{qU_0} \right]^{\frac{2}{k-2}}$$

Unlike the quadrupole trap, the well depth diminishes as the trapping voltage U_0 increases. As k gets large, $V^*(R_{\max})$ approaches

$$V^*_{k\gg 1}(R_{\max}) = \frac{m\Omega^2 r_0^2}{k^2} \frac{\eta_{\max}^2}{16}$$

showing that the well depth decreases as the square of the number of multi-poles, but increases with particle mass, trap operating frequency, and size. For higher pole traps, the well depth becomes insensitive to the trap operating voltage. This is very different behavior from a linear quadrupole trap where the transverse well depth scales as $q^2U_0^2/m\Omega^2 r_0^2$ [5].

To understand space-charge interactions, we have solved the Boltzmann equation to find the thermal equilibrium density distribution of ions at temperature T held in the pseudo-potential well of the multi-pole trap. The radial density, $n(r)$, of ions at temperature T held in the multi-pole trap is found from the Boltzmann distribution [6–8] $n(r) = n(0)\exp(-(V^*(r) + q\varphi_{sc}(r))/k_B T)$, where $-\varphi_{sc}(r)$ and $n(r)$ are related through Poisson's equation, $\nabla^2 \varphi_{sc}(r) = -qn(r)/\varepsilon_0$. This leads to the equation [2] for $n(r)$:

$$n'' + \frac{n'}{r} - \frac{n'^2}{n} - \frac{n^2}{n_0 \lambda_D^2} = -k^2(k-1)^2 \frac{n}{4\lambda_D^2} \hat{r}^{2k-4}$$

In this equation, $n_0 = 2\varepsilon_0 m\omega^2/q^2$ is the pseudo-charge density in the quadrupole trap with secular frequency ω, produced by a quadrupole trap of the same operating parameters as the multi-pole trap, and $\lambda_D^2 = k_B T/(2m\omega^2)$ is the Debye length for the ion plasma.

To compute the second-order Doppler shift for the ion-cloud density distribution, we must also know the micro-motion velocity, v, throughout the ion trap. This is given by

$$\langle v^2 \rangle = \frac{k^2}{4}\omega^2 r_0^2 \hat{r}^{2k-2}$$

where the brackets $\langle\,\rangle$ indicate time averaging over a micro-motion cycle.

It is useful to define the normalized second-order Doppler shift from the two-dimensional micro-motion versus radial position as follows:

$$\frac{-\left\langle \dfrac{v^2}{2c^2} \right\rangle}{-\dfrac{k_B T}{mc^2}} = \frac{k^2}{8} \frac{m\omega^2 r_0^2}{k_B T} \hat{r}^{2k-2} \equiv F_d^k(r)$$

Notice that the normalized second-order Doppler from the micro-motion is less than the ion thermal motion throughout most of the interior of the cloud.

Finally, we compute the total second-order Doppler from the micro-motion averaged across the ion cloud as

$$N_d^k = \frac{\int n(r) r F_d^k(r) dr}{\int n(r) r dr}$$

From this calculation, we find the total second-order Doppler shift for the trapped ions with density profile $n(r)$:

$$\frac{\Delta f}{f} = -\frac{3k_B T}{2mc^2}\left(1 + \frac{2}{3}N_d^k\right)$$

We can now evaluate this expression numerically for any multi-pole linear trap with a given total number of ions per unit length and temperature. We first note that in the limit of small ion clouds where space-charge effects are negligible ($\varphi_{sc} = 0$), N_d^k can be evaluated analytically, giving $N_d^k = 1/(k-1)$. This result can be seen more easily by use of the virial theorem. The second-order Doppler frequency shift is

$$\frac{\Delta f}{f} = \left\langle -\frac{KE}{Mc^2} \right\rangle \equiv \left\langle -\frac{KE_z + KE_{\text{secular}} + KE_{\mu\text{motion}}}{Mc^2} \right\rangle$$

The rf confinement is purely transverse so that the axial and transverse kinetic energies are independent. The kinetic energy in the micro-motion is the pseudo-potential energy $KE_{\mu\text{motion}} \equiv U_{\text{pseudo}} \propto r^{2k-2}$. Because the two-dimensional confining potential is a power law in radius, ion motion follows the virial theorem [9]. Accordingly, the time-average values of the kinetic and potential energies are related: $2\langle KE_{\text{secular}} \rangle = (2k-2)\langle U_{\text{pseudo}} \rangle$. Since each degree of freedom is assumed to have energy $k_B T/2$, $\langle KE_z \rangle = 1/2 \langle KE_{\text{secular}} \rangle = (1/2)k_B T$, and it follows that

$$\frac{\Delta f}{f} = -\frac{3k_B T}{2mc^2} \left(1 + \frac{2/3}{k-1}\right)$$

Thus, with no space-charge interaction, $N_d^k = 1/(k-1)$.

In the linear quadrupole trap with only a small number of non-interacting ions, $N_d^{k=2} = 1$. This is a consequence of the equality of the average secular energy and average micro-motion energy in a harmonic (quadrupole) trap. As space-charge interaction grows larger, $N_d = N_d^{k=2}$ increases. This number is as large as 3 for buffer-gas-cooled Hg ion clocks.

The 12-pole trap, by contrast, begins in the small cloud limit as $N_d^{k=6} = 1/5$, already 5 times smaller than in the quadrupole. Additionally, because the field-free interior volume of the multi-pole trap is much larger than the quadrupole trap with the same radius, the low-density limit is satisfied with a much larger number of ions.

II. First Multi-Pole Clock Operation

We have built a 12-pole trap (Fig. 1) along with a co-linear quadrupole trap where ions are optically pumped between periods of microwave interrogation in the 12-pole trap. Ions were loaded into the
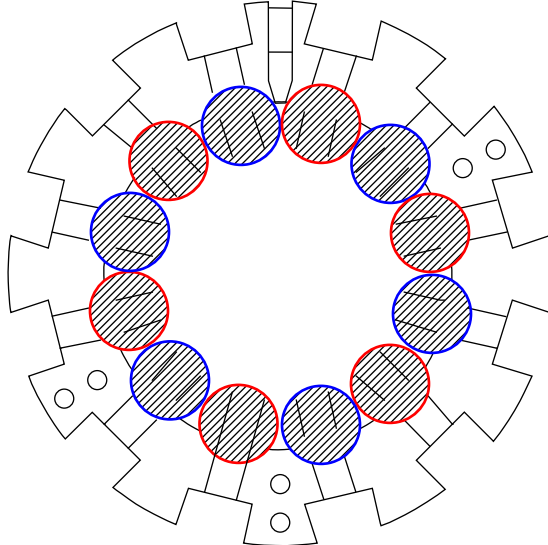

Fig. 1. The linear 12-pole trap cross-section. The inner radius from center to first contact with the rod electrodes is 5.6 mm. Microwaves at 40.5 GHz enter the trap between rods, as shown at "12 o'clock," via a small (1 x 2 mm) dielectric-filled waveguide and horn.

4

quadrupole trap, where the atomic fluorescence was measured with good signal-to-noise ratio. The ions then were electrically shuttled into the co-linear 12-pole trap and then shuttled back into the quadrupole trap, where fluorescence measurements show negligible ion loss in transport across the junction between the two traps. This also demonstrates that losses from the 12-pole trap were insignificant. This is important because the well depth of the 12-pole trap is around 0.3 eV as compared with the 3+ eV well depth of the linear quadrupole trap.

The Boltzmann equation solutions outlined above can be used to investigate the ion-cloud radial-density profile in each of the two traps involved in this 12-pole Hg$^+$ ion clock. Ions are loaded into the quadrupole trap every cycle of the measurement simultaneously with the optical pumping of the ions that were just moved into the quadrupole trap from the 12-pole trap. For a typical operating condition, $\sim 10^7$ ions are transferred back and forth in this manner. The density inside the 12-pole trap is much weaker than inside the quadrupole trap, in part because the 12-pole trap is 3.8 times the length of the quadrupole trap. The bigger reduction in density comes from the nature of the multi-pole trap, where the fields are very small until about 4.5 mm from the center. The comparison of the two profiles is shown in Fig. 2. The quadrupole trap is operated at $U_0 \sim 280$ V, while the 12-pole trap is run at $U_0 \sim 60$ V, with both at 1 MHz.

Conventional quadrupolar Hg standards developed in our laboratory show a 1 to 2×10^{-12} frequency offset as the trap is loaded with ions in order to achieve a good signal-to-noise ratio in the clock transition. The normalized micro-motion second-order Doppler shift can be in effect much "hotter" than the secular; that is, $N_d^{k=2}$ can be as large as 3. But there is some heating of the secular temperature when there is so much micro-motion with a large cloud. We have measured the sensitivity of the Hg 40.5-GHz clock resonance frequency to changes in ion number in the resonance trap. The 12-pole trap, with the greatly reduced micro-motion ($N_d^{k=6} = 1/5$), is naturally much less sensitive to such space-charge and rf-heating problems. The measured frequency pulling of the clock transition as ion number is changed in both a quadrupole trap and a 12-pole trap is shown in Fig. 3. As the end-pin voltage diminishes to less than ~ 5 V, fewer ions are held in these two linear traps. For the 12-pole trap, the half-signal point is 3 to 4 V, while the quadrupole trap reaches half-signal as the end-pin voltage falls below 5 to 6 V. This is an artifact of the electron optics and loading rates for each trap. As can be seen, the 12-pole trap is drastically less sensitive than the quadrupole trap to variations in ion number for the same large cloud
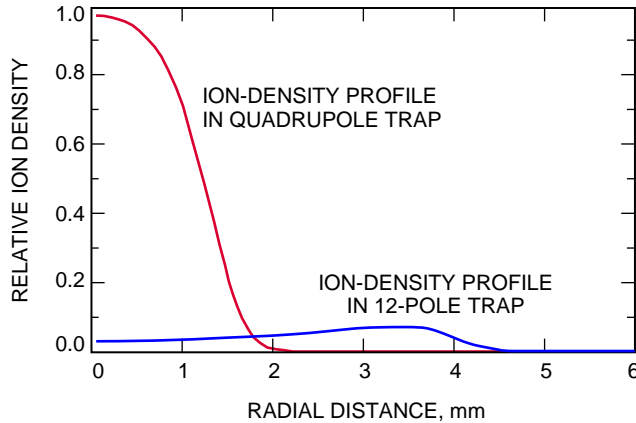

Fig. 2. The ion (radial) density distributions for ~10^7 ions in both the quadrupole and 12-pole traps. The 12-pole trap described here is ~3.8 times longer than the quadrupole trap, further reducing the ion density inside the 12-pole trap. The central density falls by ~16 as ions are shuttled into the 12-pole resonance trap.
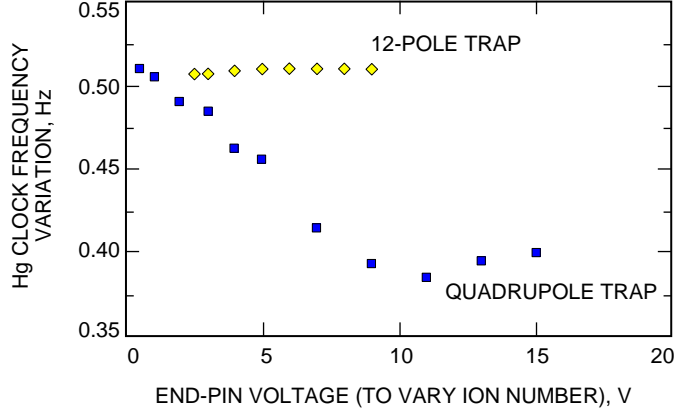
Fig. 3. Variation of the Hg clock frequency with ion number.

($\sim 10^7$ ions) conditions. In both traps, the low end-pin voltage operation has less than $\sim$5 percent of the total number of ions as the high voltage operation. In these data, the number of trapped ions is controlled by the end-pin voltage; that is, as end-pin voltage is reduced below $\sim$10 V, fewer ions are trapped. This is a consequence of loading rates and loss rates in the vicinity of the electron gun where ions are created.

The clock operation of the 12-pole trap is carried out with a 6-s Rabi pulse applied to the ions after they have been optically pumped in the quadrupole trap and then transferred into the multi-pole trap. The signal size for the resonance is $\sim$50,000 counts on the peak of the resonance curve with a background stray light level of $\sim$220,000 photon counts. The time required for a single measurement cycle is about 11 s. These parameters predict a short-term Allan deviation (limited by photon-counting statistics) of $\sim 7 \times 10^{-14}/\tau^{1/2}/\mathrm{Hz}^{1/2}$. Figure 4 shows the linear ion trap extended (LITE) 12-pole clock stability measured against a hydrogen maser, Smithsonian Astrophysical Observatory (SAO-26), demonstrating a slight degradation by the H-maser as a local oscillator. This 7-day continuous measurement of the 12-pole stability was limited by the maser frequency instabilities beyond $\sim$30,000-s averaging times. A second LITE 12-pole trap will soon be operational and will allow much lower noise-floor measurements.

The leading frequency offsets for the 12-pole configuration are listed in Table 1. Changes in these offsets will lead to clock frequency instabilities. Accuracy approaching 10^{-14} may be practical in a rack-mountable Hg clock based on the multi-pole linear trap. Use of the multi-pole linear trap has reduced the total second-order Doppler shift by almost a factor of 10. Furthermore, the space-charge-induced second Doppler has been reduced by 20 or more. This has been the largest source of potential frequency instabilities in previous lamp-based Hg frequency standards. The degree of regulation required to reach 10^{-16} stability also is shown in the table.

The ion-cloud temperature can be measured by propagating microwaves along the axis of the linear 12-pole trap as described in [6]. The 40.5-GHz transition will then be first-order Doppler broadened to

$$\delta \upsilon = 2(\upsilon_0/c)\sqrt{\frac{2k_B T \ln 2}{m}} = 2.056\sqrt{T} \text{ kHz } = 35.6 \text{ kHz}$$

for $T = 300$ K. The width of this resonance could be measured to $\sim$5 percent to determine the secular-temperature second-order Doppler offset to an uncertainty of $\sim 10^{-14}$. The ion-temperature stability may ultimately be determined by the ambient-temperature variation since the buffer gas is at that temperature. The ambient 0.1-K temperature stability requirement for 10^{-16} clock operation is readily met in most frequency-standard laboratories.
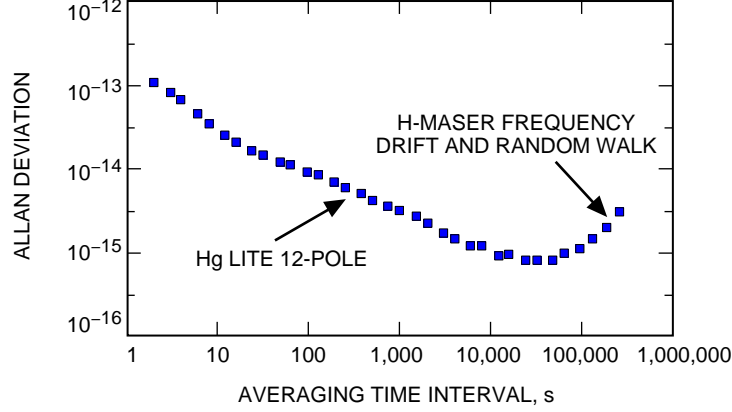
Fig. 4. Measured Allan deviation for the LITE 12-pole
Hg$^+$ ion clock versus a hydrogen maser.

Table 1. Frequency offsets for the 12-pole configuration.

Frequency offset	Magnitude	Projected absolute uncertainty	Regulation required to reach 10^{-16}
Second-order Doppler			
Secular ($\sim$300 K)	2.4×10^{-13}	1×10^{-14}	Ion temperature $\sim$0.1 K
Space-charge-induced micro-motion	2×10^{-14}	$<10^{-14}$	Ion number $\sim$0.5 percent
Second-order Zeeman (at 35 mG)	3×10^{-12}	1×10^{-14}	$\sim 5 \times 10^{-7}$ G
Helium buffer gas	1.1×10^{-13}	10^{-14}	$\sim 10^{-8}$ mBar
AC Zeeman	$<10^{-14}$	$<10^{-14}$	$\sim$1 percent

III. Summary

There has been considerable progress in the last two decades since trapped-ion standards were first realized. Clocks based on mercury ions in linear traps are already operational and support deep-space navigation in the Deep Space Network. New developments based on multi-pole traps promise the realization of small, highly stable clocks with enough accuracy to support space-borne applications. These and other emerging improvements will make future trapped-ion clocks and frequency standards available to a much larger class of applications, ranging from tests of fundamental physics to navigation on Earth and on planetary surfaces.

Acknowledgment

References

[1] D. Gerlich, "Inhomogeneous RF Fields: A Versatile Tool for the Study of Processes with Slow Ions," *Adv. Chem. Phys.*, vol. LXXXII, pp. 1–176, 1992.

[2] J. D. Prestage, R. L. Tjoelker, and L. Maleki, "Higher Pole Linear Traps for Atomic Clock Applications," *Proc. 1999 Joint EFTF/IEEE International Frequency Control Symposium*, Besancon, France, pp. 121–124.

[3] H. G. Dehmelt, "Radio-Frequency Spectroscopy of Stored Ions I: Storage," *Advances in Atomic and Molecular Physics*, vol. 3, pp. 53–72, 1969.

[4] L. S. Cutler, C. A. Flory, R. P. Giffard, and M. D. McGuire, "Doppler Effects Due to Thermal Macro-Motion in an RF Quadrupole Trap," *Appl. Phys. B*, vol. 39, pp. 251–259, 1986; also L. S. Cutler, R. P. Giffard, and M. D. McGuire, "A Trapped Mercury 199 Ion Frequency Standard," *Proc. 13th Ann. PTTI Application and Planning Meeting*, NASA Conference Publication 2220, pp. 563–578, 1981.

[5] G. R. Janik, J. D. Prestage, and L. Maleki, "Simple Analytical Potentials for Linear Ion Traps," *J. Appl. Phys.*, vol. 67, pp. 6050–6055, 1990.

[6] J. D. Prestage, R. L. Tjoelker, G. J. Dick, and L. Maleki, "Doppler Sideband Spectra for Ions in a Linear Trap," *Proc. 1993 IEEE International Frequency Control Symposium*, Salt Lake City, Utah, pp. 148–154, 1993.

[7] L. S. Cutler, C. A. Flory, R. P. Giffard, and M. D. McGuire, "Doppler Effects due to Thermal Macromotion of Ions in an rf Quadrupole Trap," *Appl. Phys. B*, vol. 39, pp. 251–259, 1986.

[8] C. Meis, M. Desaintfuscien, and M. Jardino, "Analytical Calculation of the Space Charge Potential and the Temperature of Stored Ions in an rf Trap," *Appl. Phys. B*, vol. 45, pp. 59–64, 1988.

[9] H. Goldstein, *Classical Mechanics*, Reading, Massachusetts: Adison-Wesley, 1950.